Published in final edited form as:
*Adv Mater*. 2013 February 6; 25(5): 772–776. doi:10.1002/adma.201204083.

# Transient Enhancement and Spectral Narrowing of The Photothermal Effect of Plasmonic Nanoparticles Under Pulsed Excitation

**Dr. Ekaterina Y. Lukianova-Hleb**,
Departments of Biochemistry and Cell Biology, Rice University, Houston, TX 77005 USA

**Dr. Alexey N. Volkov**,
Department of Materials Science and Engineering, University of Virginia, Charlottesville, VA 22904-4745 USA

**Dr. Xiangwei Wu**, and
Department of Head and Neck Surgery, The University of Texas, MD Anderson Cancer Center, Houston, TX 77030 USA

**Dr. Dmitri O. Lapotko**
Department of Biochemistry and Cell Biology, Department of Physics and Astronomy, Rice University, 6100 Main, MS-140, Houston, TX 77005 USA, Phone: 713-348-3708, Fax: 713-348-5154

Dmitri O. Lapotko: dl5@rice.edu

**Keywords**

plasmonic nanobubble; near-infrared; photothermal; gold nanoparticle; laser pulse

Metal plasmonic NPs are the best converters of light into heat through the mechanism of surface plasmon resonance.[1,2] This unique photothermal (PT) property was developed to allow precise manipulations of thermal energy at nanoscale through engineered plasmon resonances.[3–6] Enhancement of the PT efficacy and spectral selectivity of such engineered NPs is associated with several principal limitations. Most commonly, stationary optical excitation creates high thermal losses[7–9] that, in turn, require additional excitation energy, while the pulsed excitation involves high optical intensities that destroy NP structure that provides optical absorbance.[10–13] Spectral width of absorption spectra of single NPs is tens of nanometers at best, while random clustering of NPs further broadens their spectra to hundreds of nanometers.[2,14–16] An ability to deliver high PT efficacy with high spectral resolution and minimal thermal losses will therefore significantly improve current applications of plasmonic materials.

Until now, the PT and spectral properties of metal NPs have been set during their synthesis[2–6,17] and have been assumed to stay constant during their excitation. Unlike this stationary paradigm we considered an alternative approach based on the non-stationary excitation of NPs. We hypothesized that the absorption of a short laser pulse by a metal NP and the induced non-stationary modification of the NP would enhance optical absorbance (and hence the PT efficacy) in the narrow, nanometer-wide, spectral window. We therefore studied the PT responses of the basic and well-studied metal NPs, solid gold spheres (known

Correspondence to: Dmitri O. Lapotko, dl5@rice.edu.

for more than one hundred years as gold colloids [18]) to short laser pulses under resonant and off-resonant pulsed optical excitation, under a wide range of models and conditions that represent the current major applications of gold NPs.

Initially we analyzed individual NPs in water under the levels of laser fluence associated with the formation of vapor nanobubbles around NPs. Gold NPs were exposed to single 70 ps laser pulses at specific wavelength and fluence (Supporting Information, Figure S1A). The nanobubble lifetime was used as a PT metric. It was obtained optically through a nanobubble-specific trace, the duration of which was measured as the nanobubble lifetime (Supporting Information, Figure S1B, S2A). Spectra of the nanobubble lifetime for the single pulse excitation of 60 nm gold spheres revealed a 2 nm wide single peak at 780 nm (Figure 1A). The lifetime at 780 nm was comparable to that at 532 nm (close to plasmon resonance), while neighboring near-infrared (NIR) wavelengths returned much lower lifetimes. Contrastingly, the optical absorbance of 60 nm gold spheres at 780 nm is only about 1% of that of the same NP at 532 nm under ambient conditions.[2] Thus we observed an 88-fold amplification of PT efficacy of gold spheres at 780 nm (Table S1). This effect was stably observed in in a wide range of excitation fluences (Figure 1A, 2A). Such narrow and enhanced PT spectra (associated with optical absorbance, not scattering) had never been observed beforehand for single metal NPs.

We next varied the NP state to clusters of 5–20 aggregated NPs (Figure 1B) and water suspensions of NPs (Figure 1C) of 20, 60 and 120 nm size. Both NP states yielded the PT amplification in the range of 70–95 at the same wavelength of 780 nm and the spectral narrowing from hundreds of nanometers (for optical absorbance of NP clusters) to 3.5–4 nm (Table S1) in a wide range of excitation fluences, starting from 10–15 mJ $cm^{-2}$ (Figure 2B, C). Next, the NP environment was varied from water to living matter. Living cancer cells HN31 were targeted with 60 and 20 nm spheres conjugated to cell-specific antibody, C225[19] resulting in intracellular NP clusters.[20] In response to a single 70 ps laser pulse the cells revealed a 2 nm wide PT peak also at 780 nm with the PT amplification above 100 (Figure 1D, Table S1). At the next stage the same conjugates of gold NPs were systemically targeted *in vivo* to a tumor grown in mice with xenografted HN31 cells. The PT spectrum was obtained acoustically, since opaque tissue compromises optical detection (Figure 1D).[21] The amplitude of acoustic traces of vapor nanobubbles correlate well to optical scattering traces in NP-treated cancer cells (Supporting Information, Figure S3).[22] PT spectra of a tumor of the NP-treated and intact animals were obtained in a single laser pulse at 40 mJ $cm^{-2}$. The NP-treated tumor revealed a 3 nm wide peak at 780 nm with the PT amplification about 95 (Figure 1E, Table S1) in a wide range of the excitation fluence (starting from 20–25 mJ $cm^{-2}$, Figure 2D). The tumor of an intact animal returned zero signals under identical optical excitation (Figure 1E). Therefore, the alternative detection method demonstrated a similar effect of the PT amplification and spectral narrowing to that which was previously observed optically.

All the five models studied above, single NPs, clusters and suspensions in water and in living matter showed similar effects of the NIR amplification of the PT efficacy at the same excitation wavelength in a very narrow, nanometer wide, spectral window that is far from the typical plasmon resonance of gold spheres in the visible region (Table S1). Such narrow PT or absorption (not scattering) spectra were never observed beforehand for single or randomly clustered metal NPs. This spectral narrowing was obtained in a wide range of conditions such as optical energy (fluence) and the NP and environment properties, that usually broaden the spectral width and shift the peak wavelength of all plasmonic NPs under stationary excitation. In particular, a variation of the excitation fluence in a wide, ten-fold, range did not influence the peak wavelength and width, showing that the observed PT amplification is not threshold-specific unlike some other non-linear optical phenomena that

are energy-sensitive and can provide spectral amplification and narrowing only close to a specific energy threshold, but disappear when the excitation energy is far from the specific threshold.[23,24] Such phenomena can improve the spectroscopic techniques as was reported previously but they cannot support the energy conversion in a wide range of excitation energies as we demonstrated. Therefore, the observed effect of the non-stationary excitation of metal NPs is associated with a new but universal mechanism.

In order to understand the mechanism of the discovered effect, we performed several additional studies. Initially, we compared the PT responses of water suspension of 60 nm NPs at the resonant (532 nm) and off-resonant (780 nm) wavelengths at fluence levels below and above the nanobubble generation thresholds. Optical traces obtained at 532 nm at low fluence showed traces of another, “thermal” shape, thus demonstrating a bulk heating-cooling cycle (Supporting Information, Figure S2B). The amplitude of the thermal trace at 532 nm increased with the fluence until the onset of nanobubbles reduced the amplitude of the thermal trace (Figure 2C). This demonstrated that the NP acted as a heat source for nanobubbles. In contrast to the above, the PT responses at 780 nm showed no detectable bulk heating at the fluence level below the nanobubble generation threshold (Supporting Information, Figure S2B). Therefore, NPs apparently did not heat at 780 nm as much as at 532 nm and this corresponds to the low optical absorbance of NP at 780 nm relative to that at 532 nm.[2] At the same time we observed the relatively early onset of nanobubble generation at the low fluence of 10–15 mJ $cm^{-2}$ (Figure 2C), so that the generation of nanobubbles at 780 nm was even more efficient in the fluence range of 10 to 40 mJ $cm^{-2}$ than that at 532 nm (Supporting Information, Figure S2C and Figure 2C). These nanobubbles were apparently generated at 780 nm without thermal support from the NP, while the generation of nanobubbles at the resonant wavelength of 532 nm was thermally supported by NP (Supporting Information, Figure S2C). Therefore, the thermal energy required for the generation of nanobubble at 780 nm came from something else, but not from the parent NP. This, in turn, suggests that the observed PT amplification and ultra-narrow spectral peaks cannot be associated with the parent NP.

We hypothesize that the spectrally selective PT amplification resulted from the non-stationary formation of a transient plasmonic structure around the NP because theory does not allow such narrow (2 nm) peaks for individual NPs alone.[2,17] We excluded localized NP-induced optical breakdown (plasma) as a possible mechanism, because the employed optical fluence (10 – 100 mJ $cm^{-2}$) and intensity (< 1 GW $cm^{-2}$) were several orders of magnitude below the reported thresholds of plasma formation near the surface of gold NPs.[25,26] In addition, plasma does not have narrow optical absorbance peaks. We therefore modeled the initial temperature dynamics of a single gold 60 nm NP in water during the absorption of a single 70 ps laser pulse at 780 nm (Figure 3A). Our estimates showed that even under off-resonant excitation at 780 nm, the NP rapidly reaches the surface melting threshold of 104°C [26] in 7 ps that can therefore develop much faster than the onset of a vapor nanobubble that requires 50–100 ps.[27,28]

The surface melting of NPs was further evaluated through the TEM (transmission electron microscopy) analysis of intact (Figure 3C) and laser-exposed (Figure 3D, 3E) NPs. Exposure at the two wavelengths, 532 nm and 780 nm at the fluence of 66 mJ $cm^{-2}$ (identical to that in Figure 1A, 3A) reduced the roughness of NPs from the initial 13±6% to 4±4% for 532 nm treated NPs and 8±4% for 780 nm treated NPs. A significant reduction in the NP diameter was observed mainly for 532 nm treated NPs (53±6 nm versus 59±6 nm for intact NPs) and not for 780 nm treated NPs (58±4 nm). The obtained TEM images and their two metrics indicate that, at 780 nm, NPs experienced surface melting, while at 532 nm, the melting impact was more pronounced and showed the formation of multiple gold droplets (Figure 3D), possibly due to the higher optical absorbance at 532 nm compared to 780 nm.

Thus, theoretical and experiment data indicated that NP surface can rapidly melt under off-resonant excitation. Finally, we analyzed the influence of the pulse duration on the observed PT amplification effect. Longer, 400 ps excitation pulse of an identical fluence of 66 mJ $cm^{-2}$ reduced the nanobubble lifetime of 60 nm NPs by three-fold compared to that at 70 ps under the excitation at 532 nm (possibly due to thermal diffusion [7,21,29]) and by 60-fold at 780 nm (Figure 3F). Thus, the off-resonant PT amplification effect almost disappeared under the 400 ps excitation. Modeling of the NP temperature dynamics under excitation with 780 nm single 400 ps pulse at 66 mJ $cm^{-2}$ (Figure 3B) showed that the onset of surface melting conditions takes longer than 100 ps and thus the onset of a vapor nanobubble may occur even before surface melting. Therefore, the observed mechanism of the PT amplification involves surface melting and requires a short excitation pulse of a relatively low fluence.

This mechanism requires further studies and can be associated with a transient nanostructure with high optical absorbance at 780 nm and a nanometer-wide peak of its optical absorption spectrum. Narrow resonances in optical absorbance were observed for stationary ensembles of metal-dielectric arrays and resonators[3,4,30,31] and as fano-resonances.[32,33] In our case, the increase in optical absorbance may result from emerging melted gold nanodroplets in water vapor near the surface of the parent NP.[34,35] Unlike the resonant excitation, the off-resonant excitation does not significantly heat the parent NP due to its low optical absorbance (Figure 2C). In contrast, the laser-induced temperature of the NP will be much higher under the resonant excitation due to the maximal optical absorbance as can be seen by comparing the bulk thermal responses (Figure 2C) and NP melting under resonant (Figure 3D) and off-resonant (Figure 3E) conditions. Under the resonant excitation the development of the transient narrow spectral peak is accompanied by significant thermal modification of the parent NP as was also observed by us previously for other NPs, gold nanorods and nanoshells[29]. Thus, off-resonant excitation may be preferable for minimizing the thermal damage of parent NPs and the unwanted bulk thermal effects. Despite significant difference in the stationary optical properties of parent NPs such as solid spheres and rods and previously studied by us hollow shells[29], they all returned similar 2 – 4 nm narrow PT spectral peaks with the similar peak wavelengths in the range 770 – 790 nm under a non-stationary excitation. Therefore, a non-stationary plasmonics may be associated with the universal transient structures that can be induced around various types of NPs.

Biomedical applications of the observed effects may raise a safety concern. We therefore checked the biodamage of the irradiated living cells and tissues. The optical dose applied *in vitro* (60 mJ $cm^{-2}$ in a single pulse mode) did not compromise the viability of the cells (at 98 %) that remained close to that in intact, untreated cells (at 99 %) 72 hours after the generation of nanobubbles. Following the *in vivo* studies, we also measured the level of the surface and subcutaneous necrosis in irradiated (6±4 %) and intact (2±3 %) tumors 72 hours after laser treatment. Thus laser pulses and nanobubbles showed negligible biodamage. The optical dose applied *in vivo* (40 mJ $cm^{-2}$) was comparable to the established safety limits[36] and besides was 4–6 orders of magnitude lower than those employed in previously reported *in vivo* photothermal therapeutic effects of gold NPs.[4–6] The off-resonant excitation, in addition, reduced bulk heating thus further improving the biosafety of the observed PT effect. Furthermore, we applied gold nanospheres, the safest, FDA-approved and most easily available gold NPs, with high storage stability, ease of functionalization and a low price. In all studied cases the photothermal effect was spatially localized by a short duration of the excitation laser pulse and, in addition, by vapor nanobubble that efficiently confines the heated volume.[37] Thus, the single pulse off-resonant excitation mode is relatively safe, employs low optical doses starting from 10 mJ $cm^{-2}$ and thus can be applied to various biomedical tasks.

In conclusion, we report an approximately 100 fold transient amplification of the photothermal efficacy and the unprecedented narrowing of the photothermal spectra to 2 – 3 nm for solid gold nanospheres under the off-resonant non-stationary optical excitation at 780 nm. This amplification and spectral narrowing were achieved with a short (70 ps) laser pulse for a wide range of fluences starting from10 mJ $cm^{-2}$ and gold nanoparticle properties, such as their size, aggregation states and environments including living matter. The transient nature and high spectral selectivity of the observed effect can be associated not with the nanoparticle itself, but with the non-stationary formation of a transient nanostructure with new optical properties. Thus, the non-stationary optical excitation of metal nanoparticles can significantly improve their photothermal efficacy and spectral selectivity that can be reliably reproduced using the methodology described above. In particular, it allows the successful use of solid nanospheres, which are cheap, easily available, biologically safe and stable NPs for near-infrared applications.

## Experimental Details (See also Supplementary Information for details)

Individual solid spherical gold NPs in water were exposed to a single laser pulse of 70 ps duration at the variable wavelength (PL-2250 Ekspla laser, see Supporting Information, Figure S1A). The fluence of the laser pulse was varied below and above the threshold for the formation of a vapor nanobubble around an NP. We recently showed that such nanobubbles can be used for imaging and the characterization of the PT properties of plasmonic NPs under pulsed optical excitation [37,38]. The PT response of an NP to a single pulse was detected with several methods: (1) optically, through the nanobubble-specific scattering trace of the probe laser beam (Supporting Information, Figure S1B). The nanobubble lifetime was used as a metric for the PT efficacy of the NP [37,38]. (2) Optically, through the heating-specific refractive trace of the probe laser beam (Supporting Information, Figure S1C). The amplitude of the trace was used as a metric for the PT efficacy of the NP. (3) Acoustically, through the nanobubble-specific acoustic trace of the pressure pulse (Supporting Information, Figure S1D). The amplitude of the acoustic trace was used as a metric for the photothermal efficacy of the NP.

## Supplementary Material

Refer to Web version on PubMed Central for supplementary material.

## Acknowledgments

Authors thank Professor Stephan Link (Rice University) for helpful discussions of our results, Ms. Debra Townly (Integrated Microscopy Core at Baylor College of Medicine) for the help with TEM imaging of gold nanoparticles, and Ms. Susan Parminter for copy-editing the text. This work was partially supported by National Institute of Health, grant R01GM094816. Supporting Information is available online from Wiley InterScience.

## References

1. Mie G. Ann Phys Leipzig. 1908; 25:377.
2. Bohren, CF.; Huffman, DR. Absorption and scattering of light by small particles. Wiley Interscience; New York: 1983.
3. Yu YY, Chang SS, Lee CL, Wang CRC. J Phys Chem B. 1997; 101:6661.
4. Dickerson EB, Dreaden EC, Huang X, El-Sayed I, Chu H, Pushpanketh S, McDonald JF, El-Sayed M. Cancer Lett. 2008; 269:57. [PubMed: 18541363]
5. Khlebtsov BN, Panfilova EV, Terentyuk GS, Maksimova IL, Ivanov AV, Khlebtsov NG. Langmuir. 2012; 28:8994. [PubMed: 22404289]
6. Gobin AM, Lee MH, Halas NJ, James WD, Drezek RA, West JL. Nano Lett. 2007; 7:1929. [PubMed: 17550297]

7. Anderson RR, Parrish JA. Science. 1983; 220:524. [PubMed: 6836297]
8. Govorov A, Richardson H. Nano Today. 2007; 2:30.
9. Keblinski P, Cahill D, Bodapati A, Sullivan CR, Taton TA. J Appl Phys. 2006; 100:054308.
10. Link S, Burda C, Mohamed MB, Nikoobakht B, El-Sayed MA. J Phys Chem A. 1999; 103:1165.
11. Inasava S, Sugiyama M, Yamaguchi Y. J Phys Chem B. 2005; 109:3104. [PubMed: 16851329]
12. Hashimoto S, Werner D, Uwada T. J Photochem Photobiol. 2012; 13:28.
13. Lukianova-Hleb E, Anderson L, Lee S, Hafner J, Lapotko DO. Phys Chem Chem Phys. 2010; 12:12237. [PubMed: 20714596]
14. Myroshnychenko V, Rodríguez-Fernandez J, Pastoriza-Santos I, Funston AM, Novo C, Mulvaney P, Liz-Marzán L-M, García de Abajo FJ. Chem Soc Rev. 2008; 37:1792. [PubMed: 18762829]
15. Quinten, M. Optical properties of nanoparticle systems: Mie and beyond. Wiley-VCH Verlag GmbH & Co. KGaA; 2011.
16. Khlebtsov NG. Quant Electronics. 2008; 38:504.
17. Hartland GV. Annu Rev Phys Chem. 2006; 57:403. [PubMed: 16599816]
18. Faraday M. Philosophical Transactions of the Royal Society of London. 1857; 147:145.
19. Sharafinski ME, Ferris RL, Ferrone S, Grandis JR. Head Neck. 2010; 32:1412. [PubMed: 20848399]
20. Lukianova-Hleb EY, Belyanin A, Kashinath S, Wu X, Lapotko D. Biomaterials. 2012; 33:1821. [PubMed: 22137124]
21. Welch, AJ.; Gemert, MJC. Optical-thermal response of laser irradiated tissue. Springer; Berlin: 2011.
22. Lukianova-Hleb EY, Ren X, Zasadzinski JA, Wu X, Lapotko D. Adv Mater. 2012; 24:3831. [PubMed: 22407874]
23. Orrit M, Bernard J, Personov RI. J Phys Chem. 1993; 97:10256.
24. Demtroder, W. Laser Spectroscopy: Basic Concepts and Instrumentation. Springer-Verlag; Berlin, Heidelberg: 2008.
25. Plech A, Kotaidis V, Lorenc M, Boneberg J. Nat Phys. 2006; 2:44.
26. Plech A, Cerna R, Kotaidis V, Hudert F, Bartels A, Dekorsy T. Nano Lett. 2007; 7:1026. [PubMed: 17352505]
27. Dou YZ, Zhigilei LV, Winograd N, Garrison BJ. J Phys Chem A. 2001; 105:2748.
28. Kotaidis V, Dahmen C, von Plessen G, Springer F, Plech A. J Chem Phys. 2006; 124:184702. [PubMed: 16709126]
29. Lukianova-Hleb EY, Sassaroli E, Jones A, Lapotko DO. Langmuir. 2012; 28:4858. [PubMed: 22339620]
30. Garcia de Abajo FJ. Rev Mod Phys. 2007; 79:1267.
31. Kravets VG, Schedin F, Grigorenko AN. Phys Rev Lett. 2008; 101:087403. [PubMed: 18764660]
32. Fano U. Phys Rev. 1961; 124:1866.
33. Luk'yanchuk B, Zheludev NI, Maier SA, Halas NJ, Nordlander P, Giessen H, Chong CT. Nat Mater. 2010; 9:707. [PubMed: 20733610]
34. Yamada K, Miyajima K, Mafune F. J Phys Chem C. 2007; 111:11246.
35. Werner D, Furub A, Okamoto T, Hashimoto S. J Phys Chem C. 2011; 115:8503.
36. Laser Institute of America. ANSI Z136.1–2007. 2007.
37. Lukianova-Hleb E, Hu Y, Latterini L, Tarpani L, Lee S, Drezek RA, Hafner JH, Lapotko DO. ACS Nano. 2010; 4:2109. [PubMed: 20307085]
38. Lukianova-Hleb E, Lapotko DO. Nano Lett. 2009; 9:2160. [PubMed: 19374436]

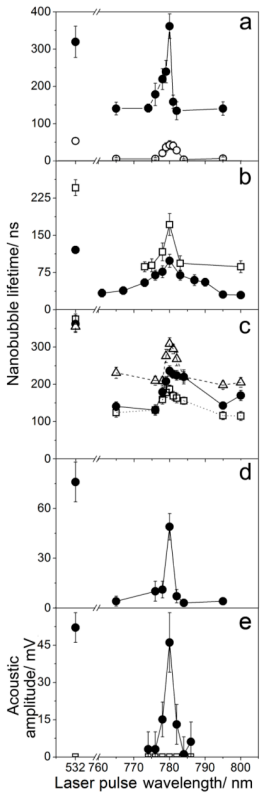


**Figure 1.**

Spectra of photothermal responses of gold spheres to 70 ps laser pulse (measured through the lifetime of vapor nanobubbles). (A) Individual gold 60 nm spheres at 66 mJ $cm^{-2}$ (*hollow dots*) and 230 mJ $cm^{-2}$ (*solid dots*) in water. (B) Clusters of 20 nm (*solid dots*) and 60 nm (*hollow squares*) spheres in water (44 mJ $cm^{-2}$). (C) Water suspensions of gold spheres with diameters of 20 nm (*dotted hollow squares*), 60 nm *(solid dots*) and 120 nm (*dashed hollow triangles*) (60 mJ $cm^{-2}$). (D) Spectra of individual cancer cells *in vitro* targeted with C225-conjugated 60 nm gold spheres (60 mJ $cm^{-2}$). (E) Spectra of acoustic responses of a tumor (*solid dots*) and intact tissue (*hollow squares*) *in vivo* in a mouse systemically treated with C225-conjugated 60 nm gold spheres (40 mJ $cm^{-2}$ ).

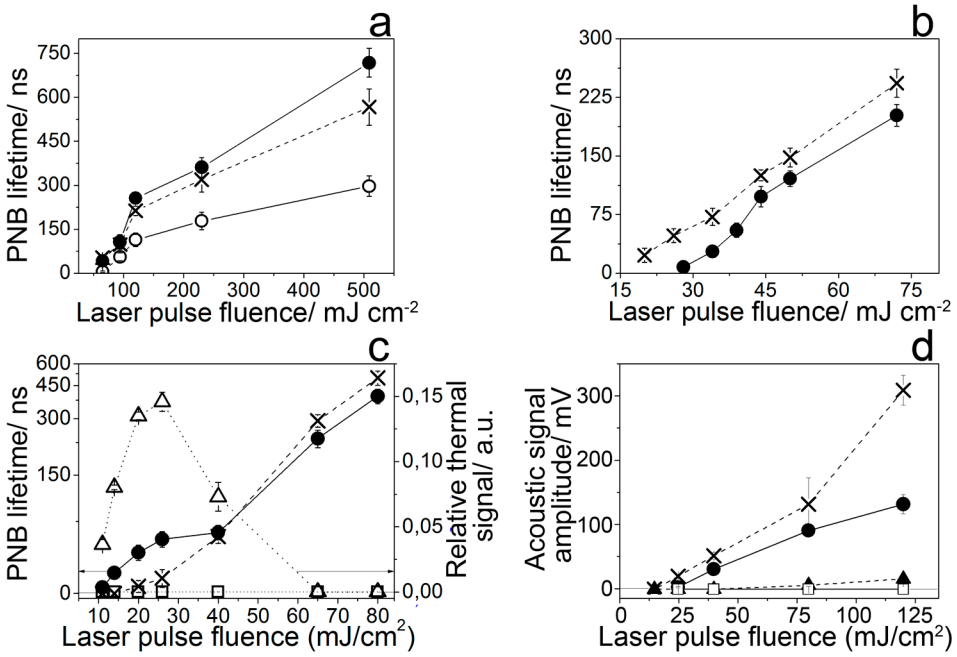


**Figure 2.**

The metrics of the photothermal responses of gold spheres as a function of the laser fluence (*dashed cross*: 532 nm, *solid circles*: 780 nm, *hollow circles*: 776 nm). (A) The nanobubble lifetime for individual 60 nm gold spheres in water. (B) The nanobubble lifetime for clusters of 60 nm gold spheres in water. (C) The nanobubble lifetime, for a water suspension of 60 nm gold spheres and the amplitude of the thermal trace (*hollow dotted triangles*: 532 nm, *hollow dotted squares*: 780 nm). (D) The amplitude of the acoustic trace for the gold NP-C225 treated mice as a function of the fluence of a single 70 ps laser pulse (*cross:* 532 nm, *solid dot*: 780 nm, NP-treated mouse: *solid dots* and intact mouse: *hollow squares (780 nm)* and *triangles (532 nm)*).

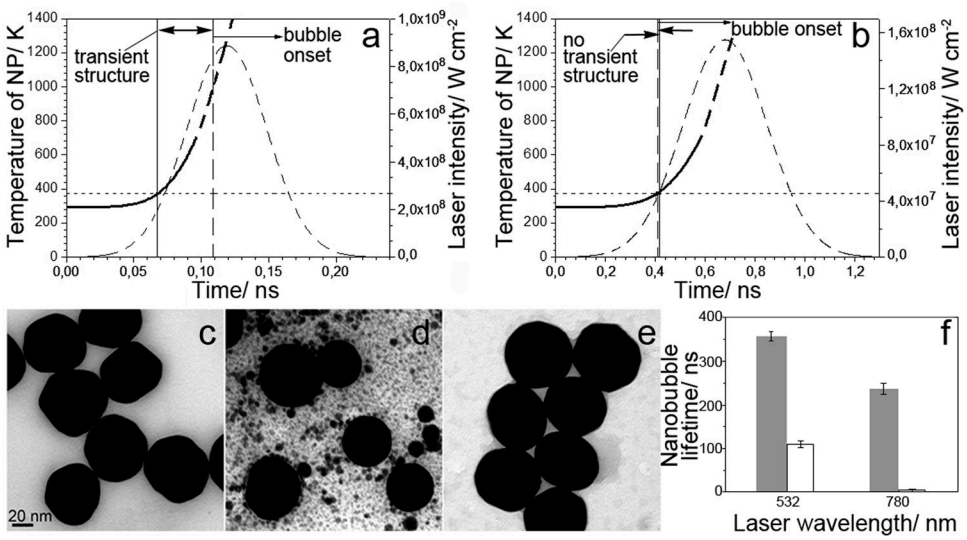


**Figure 3.**

The calculated time-course of the temperature of gold 60 nm spheres in water (*solid line*) during the absorption of a single laser pulse at 780 nm with a Gaussian temporal profile (*dashed line*) with the fluence of 66 mJ $cm^{-2}$, (A) the duration of 70 ps and (B) 400 ps. The horizontal *dotted* line shows a temperature threshold of NP surface melting. The solid vertical line indicates the potential onset of the transient structure and the dashed vertical line indicates the onset of the vapor nanobubble. Arrows show the temporal window for the transient nanostructure. Transmission Electron Microscopy (TEM) images of 60 nm gold spheres before (C) and after exposure to single laser pulses (70 ps, 66 mJ $cm^{-2}$) at 532 nm (D) and 780 nm (E); (F): comparison of the nanobubble lifetime in water suspensions of 60 nm NPs under excitation at 66 mJ $cm^{-2}$ with 70 ps (*solid bars*) and 400 ps (*hollow bars*) laser pulses at resonant (532 nm) and off-resonant (780 nm) wavelengths.